IJAE
Vol. 121, n. 3: 240-252, 2016
ITALIAN JOURNAL OF ANATOMY AND EMBRYOLOGY

Research article - Histology and cell biology

Morphological and morphometric analysis of the distal branches of the rat brachial plexus

Matthew J. Barton[1,5,*], James StJohn[1,2,5], Artiene Tatian[3], James D. Riches[4], Omar Mograby[3], David A. Mahns[3]

[1] Menzies Health Institute Queensland, Griffith University, QLD 4222, Australia; [2] Griffith Institute for Drug Discovery, Griffith University, QLD 4111, Australia; [3] School of Medicine, Western Sydney University, Penrith, NSW 2751, Australia; [4] Institute for Future Environments, Queensland University of Technology, Brisbane, QLD 4001, Australia; [5] Clem Jones Centre for Neurobiology and Stem Cell Research, Griffith University QLD 4111

Abstract

The rat brachial plexus has gained interest recently in neuro-regenerative research due to the advancement of neurosurgical equipment and techniques, but moreover in that it provides a model that can closely resemble the common peripheral nerve injuries seen in humans. The aim of this study was to provide a systematic baseline quantification for fibre type and morphology of the major terminal nerve branches of the rat brachial plexus (radial, ulnar and median) at four surgically accessible sites, through the forelimb. We applied a microstructural and immunohistological analysis of 12 rat brachial plexuses using three forms of micro-visualisation: electron microscopy; whole mount; and immunohistology. The three distal nerves studied showed a similar patterning in terms of the number and size of myelinated fibres, with all proportionally decreasing when moving distally. The fibre types of both the median and ulnar nerve appeared to be homogenously mixed throughout their trajectory, while the radial nerve had a more distinct patterning, especially distal to the elbow, with the entire nerve's main branch appearing to consist of sensory fibres only. Our microstructural analysis of the rat brachial plexus provides important normative reference data for future peripheral nerve research using the forelimb of the rat.

Key words

Brachial plexus, radial nerve, ulnar nerve, median nerve, rat.

Introduction

Peripheral nerve damage follows a large spectrum of causes, including: tumours, traumatic injuries and iatrogenic lesions (Lee and Wolfe, 2000; Campbell, 2008). These nerve injuries can result in total or partial dysfunction to sensory, motor and autonomic nerve fibres. Such injuries can lead to increased morbidity, psychosocial distress and economic burden for the patient (Campbell, 2008). Therefore, peripheral nerve injury and its ensuing repair techniques have been a persistent area of research for decades, with the ultimate objective on improving the diagnosis and subsequent reconstructive therapies. Through scientific refinement (i.e. improved microsurgical devices), nerve reconstructive surgery is now a routine practice in many trauma centres and has formed a promising translational link between nerve reconstructive surgeons and neuroscientists. Nevertheless, these translational advancements are

* Corresponding author. E-mail: m.barton@griffith.edu.au

http://www.fupress.com/ijae
DOI: 10.13128/IJAE-20273

directly dependent on the availability of experimental animal models and in recent times have seen the majority of work on rodent models. Subsequently, most peripheral nerve lesion experiments are on the rat sciatic nerve, presumably due to its larger size, relatively easy access and visualisation of nerve lesions, alongside the many standardised functional assessment tools, i.e. sciatic functional index, ankle kinematics, gait stance duration, walking tracks and toe-out angles (Bervar, 2000; Varejão et al., 2001, 2003; Couto et al., 2008; Monte-Raso et al., 2010).

Induced sciatic nerve lesions however can incite a strong propensity toward the animal developing autotomy and/or articular contractures, both causing unpredictable functional outcomes (Bertelli et al., 1995). The terminal nerves of the brachial plexus thus provides an alternative to the sciatic nerve for peripheral nerve research, and have gained more favour recently (Bertelli and Ghizoni, 2010). As a lesion model, the brachial plexus proves advantageous, as it is devoid of the post-surgical complications seen in the sciatic nerve model (Santos et al., 2007), whilst the shorter route required to regenerate axons of the brachial plexus's nerves in the forelimb relative to the sciatic nerve in the hindlimb results in faster identification of nerve regenerative outcomes (Almeida et al., 2013). Moreover, the majority of human peripheral nerve injuries impact the upper extremities, highlighting greater relevancy of forelimb nerves in experimental animal research (Bontioti et al., 2003). Finally, the common obstacles once perceived against the use of the brachial plexus's nerves, such as the small nerve sizes and the complexity of the microsurgical procedure, have become redundant due to the advancements in operating microscopes, microsurgical equipment and techniques (Siemionow and Zor, 2015). Recent developments and research into the rodent brachial plexus has additionally resulted in accepted and standardised functional/behavioural tests, i.e. toe and print length, gait analysis and horizontal ladder (Metz and Whishaw, 2002; Bontioti et al., 2003; Galtrey and Fawcett, 2007; Wang et al., 2008), alongside the well-recognised grasp test originally validated by Papalia and colleagues (Papalia et al., 2003). The development of these functional tests and behavioural tools has afforded to quantify small biomechanical changes to assess peripheral nerve regeneration. Furthermore, it is also important to quantify the anatomical and histological baseline of control nerves to ensure experimental reliability and reproducibility before undertaking any experimental interventions.

The anatomical, quantitative knowledge on the brachial plexus in the rat is heavily reliant upon the works by (Greene, 1935), which produced an ideal baseline guide to the anatomy of the forelimb and nerve mapping, however it is limited by the lack of morphometric data on the terminal branches and their fibre types. Bertelli et al. (1995) provided microsurgical mapping and identification of terminal branches. Their work however only accounted detail for the median nerve, although identifying interesting anatomical variations between rat strains. More recently, work by Santos et al. (2007) defined the morphometric dimensions of the ulnar, radial and median nerves of the rat, however provided little detail on mapping nerve fibre types, whilst Almeida et al. (2013) provided supplementary information about the blood supply to the terminal branches. We have endeavoured to provide additional baseline quantification of three main terminal nerve branches exiting the rat brachial plexus (radial, ulnar and median) at four surgically accessible sites through the forelimb. This study provides a fibre type mapping profile of these three nerves and a detailed description of their anatomical pathway.

Material and Methods

Animals and treatments

We used a total of 12 Wistar rats, with all procedures performed in accordance to animal ethics approval at both Griffith University and Western Sydney University (ESK/03/11/AEC and A8900 respectively). Male and female adults in excess of 200 g were used. Rats were first anaesthetised by isofluorane (0.5%) / O_2 mixture and then given a subcutaneous bolus of Nembutal (~1mL), until unresponsive to crude stimuli. The heart was then exposed and the animals were perfused with 50 mL of heparinised saline, followed by 300 mL of 4% paraformaldehyde. Rats were then divided into three groups:

Group 1: consisted of six rats, stained (n=3) and unstained (n=3) to determine a detailed description of each nerve's (median, ulnar and radial) anatomical pathway.

Group 2: consisted of three rats, prepared for electron microscopic analysis to quantify the number and morphology of myelinated fibres within each nerve (median, ulnar and radial) at four distinct sites through the forelimb.

Group 3: consisted of three rats, prepared for immunohistochemistry, to demonstrate the distribution of fibre types within each nerve (median, ulnar and radial) at four distinct sites through the forelimb.

Group 1: Nerve anatomic mapping

After perfusion, three animals had their right upper limb dissected under an operating microscope and each aforementioned nerve (unstained) was anatomically mapped from its origin exiting the spinal cord, moving distally to the digits. The remaining three animals had their right upper limbs removed at the axilla region and processed and stained for *in situ* whole mount visualisation using Sihler's staining procedure (Metz and Whishaw, 2002), as follows. First, each right forelimb was immersed in 4% paraformaldehyde solution for 1 month, with the solution replaced weekly. Fixed specimens were then washed under running water for 1 hour and placed in a solution containing 3% aqueous potassium hydroxide solution in 0.2 ml 3% hydrogen peroxide per 100 ml for 4 weeks, with the solution changed every 2 days. Specimens were then shifted to Sihler's solution I (1:1:6 = glacial acetic acid : glycerin : 1% aqueous chloral hydrate), which was refreshed weekly for a month. Specimens were then stained for three weeks with Sihler's solution II (1:1:6 = Ehrlich's hematoxylin : glycerin : 1% aqueous chloral hydrate). Stained specimens were then placed into Sihler's solution I, stirred lightly and terminated (~3 days) when stained nerve twigs were visible. The specimens were viewed on a light box to observe the degree of transparency. The specimens were neutralized by soaking in 0.05% lithium carbonate solution for approximately 1 hour and then washed under running water for 1 hour. Finally, the specimens were cleared with increasing concentrations of glycerine (40%, 60%, 80%, and 100%) over 24 h and photographs were taken under light microscopy.

Group 2: Nerve morphometry and morphology

The three animals in the second group, once perfused, had each nerve (median, ulnar and radial) removed at four distinct regions (brachium, elbow, wrist and digit;

refer to Fig. 1) in 10 mm segments from their right forelimb. Specimens were then fixed in 3% gluteraldehyde in 0.1M sodium cacodylate buffer overnight, post-fixed with osmium tetroxide, dehydrated and embedded in LX112 resin. 70 nm transverse sections were cut on a Leica UC7 ultramicrotome. Sections covering the entire cross section of each nerve were collected on formvar coated copper slot grids coated, post-stained with uranyl acetate and lead citrate and examined in a JEOL 1400 transmission electron microscope. All myelinated axons in each nerve were manually counted, using montages of electron micrographs by Microsoft (Redmond, WA, USA) ICE software. The cross sectional area of each nerve and measurements of myelinated fibre diameters were made on montages of electron micrographs. Diameters and areas were calculated from cross-sectional dimensions determined by Image J software (NIH, Bethesda, MD, USA). One radial nerve from the digit was discarded from the study due to poor resin infiltration, therefore an additional section was used from one of the other radial nerve blocks.

Group 3: Nerve fibre types

For immunohistochemistry, the three animals from the third group, once perfused, had each nerve (median, ulnar and radial) removed at four distinct regions (brachium, elbow, wrist and digit; see Fig. 1) in 10 mm segments from their right forelimb. Specimens were then immersed in 30% sucrose overnight 4 °C and then embedded in OCT and stored at -80 °C. Transverse sections (10 μm) were collected on a cryostat microtome. Immunohistochemistry was performed using antibodies against 1) ChAT (choline acetyltransferase) for motor fibres (1:200, Merck Millipore, Bayswater, VIC, AUS) followed by rabbit anti-goat secondary antibodies conjugated Alexa Fluor^{594} (1:400; Molecular Probes, Carlsbad, CA, USA); and 2) bIII tubulin, for all nerve fibres (1:200, AbCam, Cambridge MA, USA) followed by anti-chicken biotin (1:200, AbCam, Cambridge MA, USA) and streptavidin conjugated Alexa Fluor^{647} (1:400, Invitrogen, Carlsbad, CA, USA). Sections were then stained with 4′,6-diamidino-2-phenylindole (DAPI) and mounted with Vectashield mounting medium (Vector Laboratories Inc, Burlingame, CA, USA) and cover-slipped. Confocal images were taken using an Olympus (Tokyo, Japan) FV1000 microscope and processed by using the FV10-ASW 3.1 Viewer (Olympus) and ImageJ softwares.

Results

Nerve anatomic mapping

Median nerve. The median nerve receives a ventral branch from the roots of all vertebral levels that serve the brachial plexus (C5-T1). These roots coalesce into superior, medius and inferior truncus branches and then further diverge into two well defined branches, the fasciculus lateralis and fasciculus medialis. These latter two fasciculus branches significantly contribute to create the median nerve proper, which lies parallel and anterior to the axillary artery and anterior to the underlying and thicker radial nerve. In the brachium (Fig. 1A: M) the median nerve descends distally, lateral to the ulnar nerve and lateral and deep to the brachial artery, giving off two

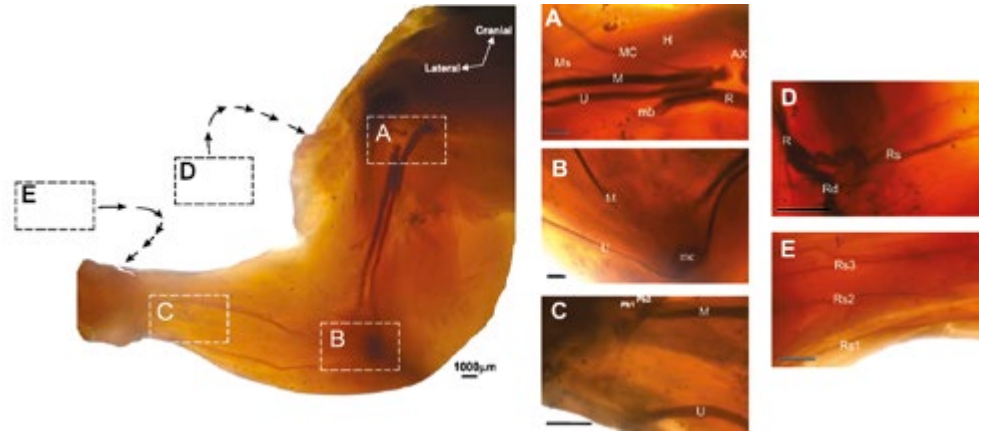

Fig. 1 Photomicrographs of the right forelimb of the rat, illustrating the terminal branches of the brachial plexus. (A) Ventral aspect of the nerves within the brachium. (B) Ventral aspect of the nerves within the cubital fossa. (C) Ventral aspect of the nerves within the wrist. (D) Dorsal aspect of the nerves within the distal brachium. (E) Dorsal aspect of the nerves within the wrist. AX: axillary nerve; H: humerus; M: median nerve; MC: musculocutaneous nerve; mb: muscular branches of the radial nerve; me: medial epicondyle; Ms: superficial branch of median nerve; Pb: palmar digital branches of median nerve; R: radial nerve; Rd: deep branch of radial nerve; Rs: superficial branch of radial nerve; U: ulnar nerve. Scale bars = 100 µm (A-E).

superficial branches (Fig. 1A: Ms) and continuing until it reaches the distal brachium, where it crosses the brachial artery from anteriorly as they enter together the hollow of elbow (cubital fossa). Upon entering the antebrachium (Fig. 1B) the median nerve runs deep to pronator teres and lateral to the brachial artery as the main trunk of the latter bifurcates into the ulnar and radial arteries. Quite proximal in the antebrachium the median nerve shoots off muscular branches to pronator teres and flexor carpi radialis, whilst a larger more distal branch enters the flexor digitorum profundus, flexor sublimis and palmaris longus. At the level of the carpal bones (Fig. 1C) the median nerve appears to give off third palmar digital branches that in turn bifurcate at the web spaces between the 1st, 2nd and 3rd digit.

Ulnar Nerve. The ulnar nerve originates from the ventral rami of C8-T1 nerve roots, which forms the truncus inferior, becomes the fasciculus medialis and then, upon entering the brachium with the brachial artery and median nerve (Fig. 1A: U), becomes the ulnar nerve. It lies deep to the brachial artery and medial to median nerve. It descends the brachium and enters the antebrachium, wrapping around the medial epicondyle (Fig. 1B: me) on the ulnar side where it immediately gives off a cutaneous branch. A muscular branch is seen to be given off in the middle of the antebrachium to flexor carpi ulnaris. En-route to the hand (Fig. 1C) the nerve, before passing deep to the pisiform bone, appears to bifurcate into a superficial and deep branch (the superficial branch was not further explored). The deep branch enters the palm surface where it appears to give off three further branches. The first branch traverses distally to the 4th digit and further bifurcates into 2 branches; one branch travels towards the interspace between the 3rd and 4th digit and the second to the 4th digit.

The second branch emerges posteriorly and appears to contribute innervation to the hypothenar musculature. The 3rd and final branch moves laterally and bifurcates into three branches presumably innervating the lumbricals and adjacent interossei.

Radial Nerve. he radial nerve receives a ventral branch from the roots of all vertebral levels, which coalesce into superior, medius and inferior truncus branches, all of which contribute a posterior branch to form a large fasciculus posterior. Both the radial and axillary nerve arises from the fasciculus posterior. The radial nerve enters the brachium between the epitrochlearis and the long and medial heads of triceps brachii (Fig. 1A: R) and enters them. Curving around the humerus towards its lateral part it can be seen to give off numerous muscular branches (Fig. 1A: mb) to the brachialis and lateral head of triceps brachii. At the lateral epicondyle of the elbow (Fig. 1D) the radial nerve divides into a superficial (Fig. 1D: Rs) and a deep branch (Fig. 1D: Rd) entering the remaining muscles in the antebrachium. The superficial branch travels distally to reach the wrist where it terminates into three branches (Fig. 1E), the largest of which (Fig. 1E: Rs1) continues distally and bifurcates over the second digit into three branches. The second digit appears to receive one branch which enters the web space between it and the 1st digit, innervating its lateral side. The second branch enters the web space between the 2nd and 3rd digit innervating the medial side of the 2nd digit and the lateral side of the 3rd. The third branch enters the web space between the 3rd digit and 4th digit, innervating the medial side of the 3rd and the lateral side of the 4th digit.

Nerve morphology and morphometry. The brachial plexus in all animals studied was composed of the ventral branches of C5-T1 and all nerves included in the study showed a good preservation of structures. Table 1 provides morphometric data obtained from the three nerves (median, ulnar and radial) in each respective segment (brachium, elbow, wrist and digit). In the brachium, the median nerve was the largest in diameter (740 mm), followed by the radial and ulnar nerves (661 mm and 480 mm respectively; Table 1). The radial nerve in the brachium had the least number of myelinated fibres (1585), compared with the median (2404) and ulnar (2301) nerves. At this level in the forelimb the radial nerve possessed a larger mean diameter of its axons (5.7 mm), compared with the median and ulnar nerves (5.2 mm and 4.7 mm respectively), whilst comprising a greater relative myelin area (fibre area minus axon area = 61.8 mm^2) relative to the median and ulnar nerves (51.6 mm^2 and 39.7 mm^2 respectively; Table 1 and Fig. 2).

At the elbow, the median nerve again was the largest in diameter (420 mm) and number of myelinated fibres (2072), followed by the ulnar and radial nerves (323 mm; 1211 and 189 mm; 329 respectively). However, similarly to the findings in the brachium, the radial nerve possessed the greatest mean diameter (4.9 mm) and average of myelin area (35.8 mm^2) of its axons, compared with the median (3.4 mm and 28.1 mm^2) and ulnar (3.5 mm and 24.7 mm^2) nerves (Table 1 and Fig. 2).

The tract between the elbow and wrist saw the ulnar nerve become the largest nerve in diameter (281 mm) and quantity of myelinated fibres (869), followed by the median (242 mm and 589 myelinated fibres) and radial (156 mm and 249 myelinated fibres) nerves (Table 1 and Fig. 3). Also at the wrist, the ulnar nerve possessed the greatest mean diameter (4.08 mm) and myelin area (29.9 mm^2) of its axons, relative to

Table 1 – Morphometric data for each of the four segments for the median, ulnar and radial nerves.

	Median				Ulnar				Radial			
	Brachium	**Elbow**	**Wrist**	**Digits**	**Brachium**	**Elbow**	**Wrist**	**Digits**	**Brachium**	**Elbow**	**Wrist**	**Digits**
Nerve												
Area (mm^2)	0.43 ± 0.08	0.14 ± 0.03	0.05 ± 0.01	0.04 ± 0.01	0.18 ± 0.05	0.08 ± 0.02	0.06 ± 0.02	0.02 ± 0.01	0.35 ± 0.13	0.03 ± 0.06	0.02 ± 0.06	0.02 ± 0.06
Diameter (mm)	740.3 ± 67.07	420.95 ± 57.93	242.78 ± 29.25	209 ± 42.27	480.19 ± 65.78	322.85 ± 52.71	281.51 ± 37.27	150.52 ± 19.27	661.15 ± 120.72	189.02 ± 19.64	155.55 ± 26.67	142.21 ± 25.56
Myelinated fibres												
Number	2404 ± 196	2072± 195	589 ± 91	422 ± 23	2301 ± 235	1211 ± 259	869 ± 18	167 ± 14	1585 ± 186	329 ± 29	249 ± 29	171 ± 16
Axon: mean diameter (mm)	5.17 ± 0.37	3.43 ± 0.54	3.74 ± 0.2	3.86 ± 0.22	4.73 ± 0.25	3.47 ± 0.24	4.08 ± 0.19	4.44 ± 0.54	5.72 ± 0.23	4.87 ± 0.1	3.54 ± 0.67	3.3 ± 0.66
median diameter (mm)	4.51	3.27	3.73	4.04	4.57	3.43	4.04	4.37	5.37	5.11	3.42	3.32
unimodal distribution	No	No	No	Yes	No	No	No	Yes	No	No	Yes	Yes
Fibre: mean diameter (mm)	9.04 ± 0.45	6.56 ± 0.75	6.37 ± 0.63	6.0 ± 0.43	8.09 ± 0.35	6.39 ± 0.46	7.16 ± 0.48	6.95 ± 0.47	10.0 ± 0.42	8.09 ± 0.36	6.08 ± 0.99	5.51 ± 0.96
median diameter (mm)	8.43	6.43	6.58	6.43	8.0	6.46	7.39	7.08	9.77	8.55	6.02	5.58
unimodal distribution	No	No	No	Yes	No	No	Yes	Yes	No	No	Yes	Yes
Fibres per mm^2	5591	14800	11780	10550	12783	15138	14483	8350	4529	10967	12450	10688
Myelin area per fibre (mm^2)	51.6 ± 4.67	28.13 ± 6.23	23.88 ± 5.9	18.68 ± 2.93	39.68 ± 3.26	24.74 ± 2.96	29.85 ± 5.08	24.99 ± 2.34	61.8 ± 5.74	35.84 ± 5.47	21.9 ± 6.1	17.34 ± 5.62

Data are expressed as median (where indicated), mean, or mean ± standard deviation.

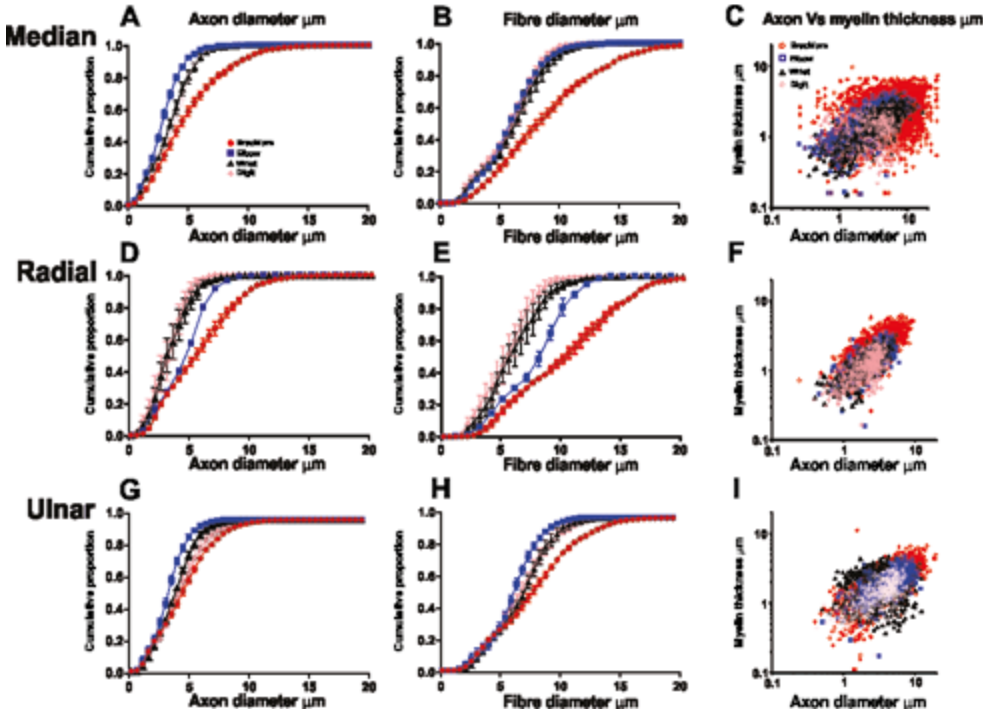

Fig. 2 Cumulative proportion of the axon and fibre diameters and regression analysis for the relationship between myelin thickness and axon diameter for (A-C) median; (D-F) radial and (G-I) ulnar nerves at each of the four analysed segments: brachium (red), elbow (blue), wrist (black), digit (pink).

the median (3.7 mm and 23.9 mm^2) and radial (3.5 mm and 21.9 mm^2) nerves (Table 1 and Fig. 2). Moreover, at the level of the wrist the radial nerve's axon and fibre diameters were seen to be uniformly distributed for the first time since nerve origin, while both the median and ulnar nerve's distributions remained bimodal (Fig. 2 and Table 1).

Finally within the paw (digit), all three nerves followed a unimodal distribution pattern in both fibre and axon diameters (Table 1 and Fig. 2). The median nerve was the largest in its diameter (209 mm), followed by the ulnar and radial nerves (151 mm and 142 mm respectively). The median nerve also had the greatest quantity of myelinated fibres (422), compared with the radial (171) and ulnar (167) nerves (Table 1). The ulnar nerve possessed the greatest mean diameter (4.4 mm) and average myelin area (25 mm^2) of its axons, compared with the median (4.7 mm and 18.7 mm^2) and radial (3.3 mm and 17.3 mm^2) nerves (Table 1 and Fig. 2).

Nerve fibre types. Transverse sections immunostained for bIII-tubulin (all fibres) and ChAT (motor) produced distinct patterning of the fibre population within the three nerves throughout their trajectory. At the level of the brachium (Fig. 3), the three nerves showed colocalised molecular expression of both aforementioned markers within the larger fibres homogenously, whilst the intermediate and smaller fibre

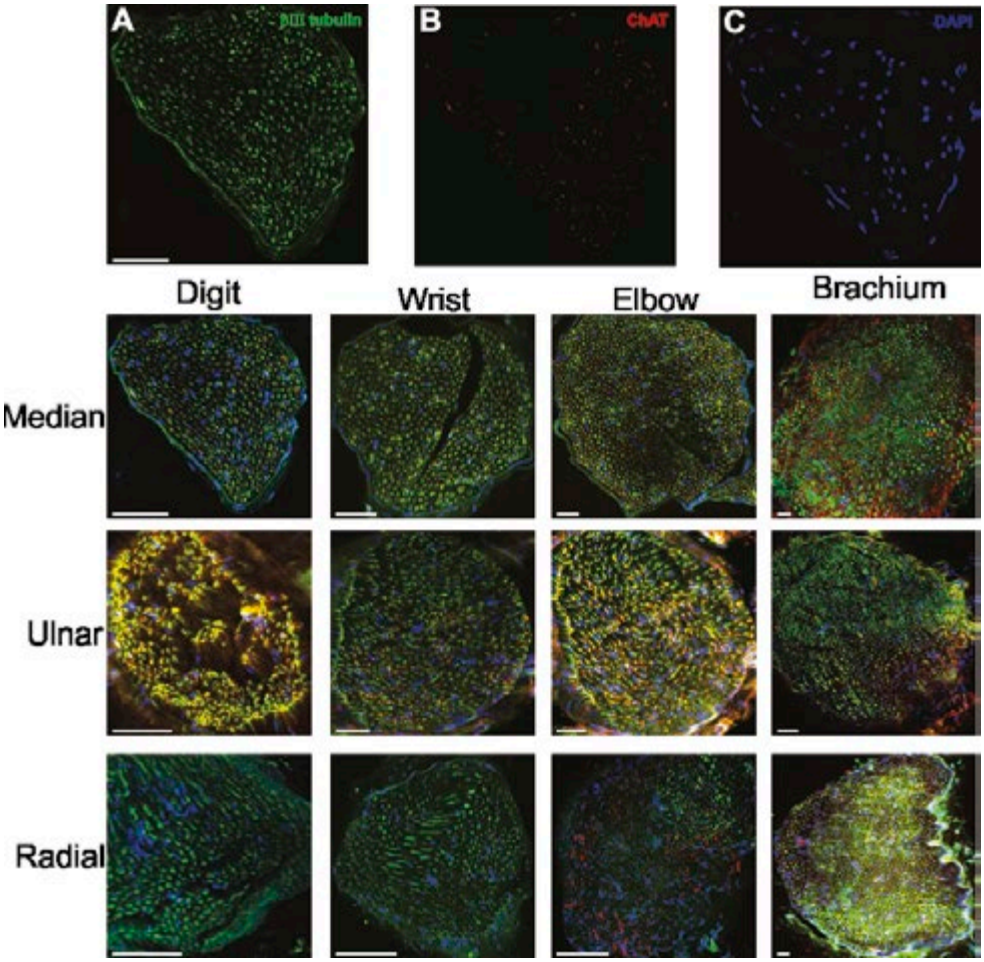

Fig. 3 Photomicrographs of immunostained transverse sections of the four segments through the median, ulnar and radial nerves respectively. (A) Digital median nerve section, stained with anti-bIII tubulin. (B) Digital median nerve section, stained with anti-ChAT. (C) Digital median nerve section, stained with DAPI. The remaining panels are merged transverse sections, stained with the three aforementioned antibodies, of the four segments through the median, ulnar and radial nerves respectively. Scale bars = 50 μm.

populations appeared ChAT negative. This homogenous patterning appeared alike within the elbow sections for both the median and ulnar nerves, and the radial nerve displayed colocalised fibres immediately preceding the nerve's bifurcation into its deep and superficial branches (Fig. 1D). The largest of the superficial radial nerve branches (Fig. 1D: Rs), that were immunostained (Fig. 3) from the elbow through to the wrist (Fig. 1E: Rs1) and beyond into the hand, all appeared to be ChAT negative. This was at variance with the median and ulnar nerves, both of which continued to show a non-uniformed colocalised patterning, as seen in the elbow and brachium

sections, although the ulnar nerve at the digit did appear to strongly colocalise both markers (Fig. 3).

Discussion

In rats, the sciatic nerve is undoubtedly the most examined in reference to nerve injuries, regeneration and pathologies, and the brachial plexus and its distal terminal branches are anatomically very similar to humans (Bertelli et al., 1995; Ozbag et al., 2009) and clinically more relevant than the sciatic nerve in terms of the injuries typically seen in humans. Nevertheless, descriptive data of the terminal nerve branches of the rat brachial plexus is currently scant, and what is reported are predominately control data limited by their association to nerve injuries or pathologies, as tabulated by Santos et al. (2007). Accordingly, the present study was designed to provide normative baseline data for future peripheral nerve research on the fibre types, morphology and morphometry of three large terminal branches of the brachial plexus (median, ulnar and radial) at four different surgically accessible locations in the rat.

As reported in humans, present findings demonstrate that the brachial plexus in the rat originates from the C5-C8 and T1 ventral branches, although in 60-65% of cases, a C4 contribution has been reported in both rodent and humans (Greene, 1935; Bertelli et al., 1995; Ozbag et al., 2009; Angelica-Almeida et al., 2013). The T2 ventral root has been reported to intermittently (~30%) contribute to the brachial plexus in humans, which is not unanimously accepted for the rat (Bertelli et al., 1995; Ozbag et al., 2009; Angelica-Almeida et al., 2013).

The median nerve in the rat is a mixed nerve, providing pronation, wrist and finger flexion whilst transporting cutaneous sensations from the medial brachium, antebrachium and lateral palm. In contrast to that seen in humans, we found two superficial branches that came off the median nerve in the brachium, which we presume are the medial brachial and antebrachial cutaneous nerves, both of which typically enter the medial fasciculus rather than median nerve in humans (Tubbs et al., 2015). The morphometric data for the rat median nerve in the brachium, elbow and wrist follow a bimodal fibre diameter distribution. This pattern of distribution was as a consequence of the nerve's branching, most notably in the antebrachium. Here we observed a ~45% decrease in the nerve's diameter between the brachium and elbow, compared with only ~12% in humans (Tubbs et al., 2015), and a 21% fibre per mm^2 reduction between the elbow and wrist, whilst the size of nerve fibres and axons decreased proportionally throughout the limb into the digits, where the distribution was seen to be unimodal.

The ulnar nerve in the rat is the terminal branch of the medial fasciculus and, as in the human, it is a mixed nerve, which innervates one and a half of the extrinsic flexor muscles within the antebrachium and much of the intrinsic finger flexors of the paw (hand) (Papalia et al., 2006), whilst carrying sensory information from the 4^{th} and 5^{th} digit. Consistent with what happens in humans, we found no branching of the nerve in the brachium. The whole nerve diameter only decreased by ~33% between the brachium and distal elbow, although the myelinated fibre count decreased by over 50%, distal to the medial epicondyle (Table 1). This suggests the connective tissue proportion of the nerve must have increased over this aforemen-

tioned course, as the mean axon diameter and myelin density both decreased (Table 1). This paradox is similar in humans, which sees negligible branching over the same trajectory, however the nerve diameter actually increases by ~12% (Tubbs et al., 2015). Presumably, in both human and rodents, as the ulnar nerve approaches the elbow for its vulnerable traverse around the medial epicondyle, which is a common site for nerve entrapment and pathology, it intrinsically gains a degree of protective connective tissue between the mid-humerus and the distal end of the cubital tunnel (Cartwright et al., 2008), where it appears to give its first significant branch. As the median nerve, the ulnar nerve in the brachium, elbow and wrist followed a bimodal fibre diameter distribution. Once entering the paw however, the diameter distribution was seen to be more uniform, with the mean fibre and axon diameters larger than those at the elbow, with the myelin density being comparable. It is conceivable that the deep ulnar nerve digital branch we examined contained predominantly motor fibres, as it proportionally comprised of a greater population of larger diameter fibres, compared with that at the elbow. A finding that is consistent with our immunohistochemical results, where the marker for motor fibres (ChAT) was strongly expressed. Compared with humans, the deep digital branches of the ulnar nerve are considered primarily motor, thus supplying the intrinsic muscles of the hand and including only a small population of fibres for cutaneous sensation (Tubbs et al., 2015).

The radial nerve is generally considered the largest branch of the brachial plexus and thus a terminal continuation of the posterior fasciculus, which receives contributions from each ventral ramus of C5-T1 roots. This nerve in the rat is a mixed nerve, providing supination, wrist and finger extension, whilst carrying cutaneous sensations from the dorsal elbow, antebrachium and lateral paw. The consistent decrease in diameter and myelinated fibres from the brachium to the elbow presently observed is likely due to its extensive branching in the brachium for both motor and sensory innervation alike, which is in contrast with that seen for the median and ulnar nerves. Similarly in humans, the radial nerve sees a ~70% reduction in its diameter and ~60% decrease in myelinated fibres over the same aforementioned trajectory (Bonnel, 1984; Chentanez et al., 2010; Tubbs et al., 2015). The superficial continuation of the radial nerve after its bifurcation, to the wrist and beyond, saw little change in regard to whole nerve diameter, fibre count and morphometry. Over this distance, the distribution of fibres remained consistently unimodal and appeared to be entirely sensory, based on the immunohistochemical results. Furthermore, when compared with humans, the superficial radial nerve had a remarkably similar mean fibre and axon diameters at the wrist: 6.32 mm (human) to 6.02 mm (rat) and 4.44 mm (human) and 3.42 mm (rat) respectively (Chentanez et al., 2010). However, huge discrepancies were seen in human nerves based on which side of the body the nerve was analysed, which is hypothesised to be due either to previous trauma or dissimilar branching due to handedness (Chentanez et al., 2010).

For all three nerves, the widest brachial segment diameters were those of the median nerves, followed by the radial and ulnar nerves, which was consistent with Bertelli et al. (1995), although Santos et al. (2007) found that the radial nerve was the largest of the three, a finding that is more consistent with what is seen in humans (Tubbs et al., 2015). In the distal sections, the ulnar nerve possessed the greatest diameter compared with the other two nerves. The radial nerve appeared to consist entirely of unimodally distributed sensory fibers, unlike the mixed fibre bimodal

arrangement of the median and ulnar nerves. This latter variance is related to the motor fibers that innervate the intrinsic hand muscles, predominately by the ulnar nerve and to a lesser degree by the median nerve; these morphometric findings were reinforced by the immunohistochemical results. However, one of the main limitations of the study was that the immunohistochemistry results were not quantitative and that further detail is required about sensory and autonomic fibres, nevertheless the provided knowledge is of great potential use.

Conclusion

The anatomical similarity of the brachial plexus and its distal branches between the rat and humans makes it possible to prefer this animal model for peripheral nerve injury and regeneration studies. Thus, this microscopic investigation on the rat's brachial plexus establishes a broad baseline of normative data for future comparisons in studies on injuries or induced pathology.

Acknowledgments

The authors thank Mr Susitha Premarathne, Dr Erika Lovas and Ms Mary Clarke for their technical assistance. Funding was by an internal Griffith Health Institute grant.

References

Angelica-Almeida M., Casal D., Mafra M., Mascarenhas-Lemos L., Martins-Ferreira J., Ferraz-Oliveira M., Amarante J., Goyri-O'Neill J. (2013) Brachial plexus morphology and vascular supply in the Wistar rat. Acta Med. Port. 26: 243-250.

Bertelli J.A,. & Ghizoni, M.F. (2010) Nerve root grafting and distal nerve transfers for C5-C6 brachial plexus injuries. J. Hand Surg. 35: 769-775.

Bertelli J.A., Taleb M., Saadi A., Mira J.-C., Pecot-Dechavassine M. (1995) The rat brachial plexus and its terminal branches: An experimental model for the study of peripheral nerve regeneration. Microsurgery 16: 77-85.

Bervar M. (2000) Video analysis of standing - an alternative footprint analysis to assess functional loss following injury to the rat sciatic nerve. J. Neurosci. Methods 102: 109-116.

Bonnel F. (1984) Microscopic anatomy of the adult human brachial plexus: an anatomical and histological basis for microsurgery. Microsurgery 5: 107-118.

Bontioti E.N., Kanje M., Dahlin L.B. (2003) Regeneration and functional recovery in the upper extremity of rats after various types of nerve injuries. J. Periph. Nerv. Syst. 8: 159-168.

Campbell W.W. (2008) Evaluation and management of peripheral nerve injury. Clin. Neurophysiol. 119: 1951-1965.

Cartwright M.S., Passmore L.V., Yoon J.S., Brown M.E., Caress J.B., Walker F.O. (2008) Cross-sectional area reference values for nerve ultrasonography. Muscle Nerve 37: 566-571.

Chentanez V., Agthong S., Huanmanop T., Pairoh S., Kaewsema A. (2010) Morphometric analysis of the human superficial radial nerve. Anat. Sci. Int. 85: 167-170.

Couto P.A., Filipe V.M., Magalhães L.G., Pereira J.E., Costa L.M., Melo-Pinto P., Bulas-Cruz J., Maurício A.C., Geun, S., Varejão A.S.P. (2008) A comparison of two-dimensional and three-dimensional techniques for the determination of hindlimb kinematics during treadmill locomotion in rats following spinal cord injury. J. Neurosci. Methods 173: 193-200.

Galtrey C.M., Fawcett J.W. (2007) Characterization of tests of functional recovery after median and ulnar nerve injury and repair in the rat forelimb. J. Peripher. Nerv. Syst. 12: 11-27.

Greene E.C. (1935) Anatomy of the rat. T. Am. Philosoph. Soc. 27: iii-370.

Lee S.K., Wolfe S.W. (2000) Peripheral nerve injury and repair. J. Am. Acad. Orthop. Surg. 8: 243-252.

Metz G.A., Whishaw I.Q. (2002) Cortical and subcortical lesions impair skilled walking in the ladder rung walking test: a new task to evaluate fore- and hindlimb stepping, placing, and co-ordination. J Neurosci. Methods 115: 169-179.

Monte-Raso V.V., Barbieri G., Mazzer N., Fonseca M.D.C.R., Barbieri C.H. (2010) A new treadmill-type motorized walking belt machine for video recording of the rat's gait and sciatic functional index measurement. A comparative study with other methods. J. Neurosci. Methods 189: 23-29.

Ozbag D., Gumusalan Y., Bakaris S., Ciralik H., Senoglu M., Kalender A. (2009) Morphologic and morphometric investigation of plexus brachialis in rat. Int. J. Exp. Clin. Anat. 3: 21-28.

Papalia I., Tos P., Stagno D'alcontres F., Battiston B., Geuna S. (2003) On the use of the grasping test in the rat median nerve model: a re-appraisal of its efficacy for quantitative assessment of motor function recovery. J. Neurosci. Methods 127: 43-47.

Papalia I., Tos P., Scevola A., Raimondo S., Geuna S. (2006) The ulnar test: a method for the quantitative functional assessment of posttraumatic ulnar nerve recovery in the rat. J. Neurosci. Methods 154: 198-203.

Santos A.P. Suaid, C.A. Fazan V.P.S., Barreira A.A. (2007) Microscopic anatomy of brachial plexus branches in Wistar rats. Anat. Rec. 290: 477-485.

Siemionow M., Zor F. (2015). Microsurgical techniques in reconstructive surgery. In: Siemionow M. Z. (Ed.) Plastic and Reconstructive Surgery. Springer, London.

Tubbs R.S., Rizks E., Shoja M.M., Loukas M., Barbaro M., Spinner R.J. (2015) Nerves and Nerve Injuries. Vol 1: history, embryology, anatomy, imaging, and diagnostics. Academic Press, London.

Varejão A.S.P., Meek M.F., Ferreira A.J.A., Patrício J.A.B., Cabrita A.M.S. (2001) Functional evaluation of peripheral nerve regeneration in the rat: walking track analysis. J. Neurosci. Methods 108: 1-9.

Varejão A.S.P., Cabrita A.M., Geuna S., Melo-Pinto P., Filipe V.M., Gramsbergen A., Meek M.F. (2003) Toe out angle: a functional index for the evaluation of sciatic nerve recovery in the rat model. Exp. Neurol. 183: 695-699.

Wang H., Spinner R.J., Sorenson E.J., Windebank A.J. (2008) Measurement of forelimb function by digital video motion analysis in rat nerve transection models. J. Periph. Nerv. Syst. 13: 92-102.